

**KERNFORSCHUNGSZENTRUM
KARLSRUHE**

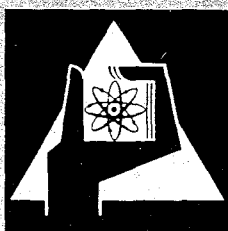
September 1968

KFK 959

Institut für Angewandte Kernphysik
Zyklotron-Laboratorium

Fast Neutron Time-of-Flight Spectrometer Used with the
Karlsruhe Isochronous Cyclotron

S. Cierjacks, B. Duelli, P. Forti, D. Kopsch, L. Kropp,
M. Lösel, J. Nebe, H. Schweickert, H. Unseld



GESELLSCHAFT FÜR KERNFORSCHUNG M. B. H.
KARLSRUHE

Fast Neutron Time-of-Flight Spectrometer Used with the Karlsruhe Isochronous Cyclotron

S. CIERJACKS, B. DUELLI,* P. FORTI, D. KOPSCH, L. KROPP, M. LÖSEL, J. NEBE,
H. SCHWEICKERT, AND H. UNSELD

*Institut für Angewandte Kernphysik and Zyklotron-Laboratorium Kernforschungszentrum Karlsruhe,
Karlsruhe, Germany*

(Received 17 May 1968)

A high resolution, fast neutron, time-of-flight spectrometer used for neutron energies between about several hundred kiloelectron volts and 30 MeV is described. A 1 nsec neutron pulse occurring with a repetition rate of 20 kc is obtained with a novel "bunching deflection" system operating on the internal beam of the fixed energy Karlsruhe isochronous cyclotron. By the timing of the neutrons over a 57 m flight path a resolution of 0.025 nsec/m at optimum was obtained. Detector counts are accumulated in a 2×8000 channel time analyzer system with 1 nsec channel width. A planned flight path of 180 m and an increase of the repetition rate from 20 kc at present to 200 kc is expected to provide further improvements of the spectrometer.

INTRODUCTION

AT the EANDC Conference on the Study of Nuclear Structure with Neutrons, held at Antwerp in 1965,¹ and some later conferences,²⁻⁴ descriptions of the spectrometer which was being developed for use with the Karlsruhe isochronous cyclotron were first presented. This apparatus was designed for high resolution, neutron time-of-flight experiments in the energy region of fast neutrons. The spectrometer in its first stage of development has been in operation for 2 yr, and till now has been used mainly for neutron transmission experiments.

I. "DEFLECTION BUNCHING" SYSTEM

A. Problems

Neutron time-of-flight experiments are greatly facilitated by the high average beam current and the small pulse width of a few nanoseconds of the microstructure pulses from sector-focused cyclotrons. With these accelerators beam intensities at relativistic energies are enhanced by a factor of about 100 compared with synchrocyclotrons, which operate in the same energy range (10 to several 100 MeV). In addition, the microstructure pulse width in a sector-focused cyclotron is much smaller (at maximum up to one order of magnitude).⁵ Unfortunately, isochronous cyclotrons run continuously with a microstructure pulse repetition rate of 10-30 Mc, which is far too high in view of frame overlap problems. Reducing the repetition rate by deflection of single microstructure pulses would be an un-

desirable sacrifice in intensity; in addition, this type of a deflection system could in our case only work on the extracted beam.

It is, however,⁶ possible to avoid the frame overlap problem while largely preserving the high average neutron intensity available from the isochronous cyclotron. For the described spectrometer this is done with a novel "deflection bunching" system operating on the internal beam. With this system the repetition rate is reduced from 33 Mc to 20 kc while the average neutron intensity is only reduced by a factor of about 30 at present. But this factor of 30 is not a true limit; a factor of 3 can be obtained, as will be shown in Sec. IV.

B. Principles of Operation

The reduction of pulse repetition rate and "bunching" is accomplished with two coupled pairs of electrostatic deflection plates. The principle of operation⁷ is shown in Fig. 1. In the normal continuous operation of our isochronous cyclotron, three ion bunches per revolution cycle are delivered from the source because acceleration is accomplished in the third harmonic mode. Both deflection systems are used for axial beam deflection. One deflector, which is located near the center of the machine, is used for a twofold purpose: (i) to eliminate two out of three microstructure pulses by deflection to a beam stop and (ii) to form ion bunches of several microsecond duration (each consisting of about 50 microstructure pulses) with a repetition rate of 20 kc.

Both conditions can be fulfilled by an appropriate deflection voltage which is indicated schematically in the

* Now at Oak Ridge Natl. Lab., Oak Ridge, Tenn.

¹ S. Cierjacks and K. H. Beckurts, *International Conference on the Study of Nuclear Structure with Neutrons, Antwerp, July 1965*, M. Neve de Mevergnies, P. van Asche, and J. Vervier, Eds. (EANDC Rep., EANDC-50-S, 1965), Vol. II, Paper 157.

² S. Cierjacks, *Physik. Verhandl.* **17**, 1 (1966).

³ S. Cierjacks, B. Duelli, L. Kropp, M. Lösel, H. Schweikert, and H. Unsel, *International Conference on Isochronous Cyclotrons, Gatlinburg, Tennessee, May 1966*, IEEE Trans. NS-13, No. 4, 353 (1967).

⁴ S. Cierjacks, P. Forti, L. Kropp, and H. Unsel, *Seminar on Intense Neutron-Sources, Santa Fé, September 1966* (TID-4500, 1966), p. 589.

⁵ *Isochronous Cyclotrons 1966, Status and Progress Summaries, Gatlinburg, Tennessee, May 1966*, IEEE Trans. NS-13, No. 4, 417 (1966).

⁶ Another possibility, as shown by Brückmann *et al.* [*Nucl. Instr. Meth.* (to be published)] is the use of a recoil proton telescope as a neutron detector where the proton energy is measured simultaneously with the neutron time of flight. Evaluating both the pulse height and the time-of-flight information allows one to determine the "gross" and "fine" neutron energy and thus to unscramble frame overlap to a considerable degree.

⁷ B. Duelli and G. Ries, *European Colloquy on AVF Cyclotrons, Eindhoven, April 1965* (unpublished).

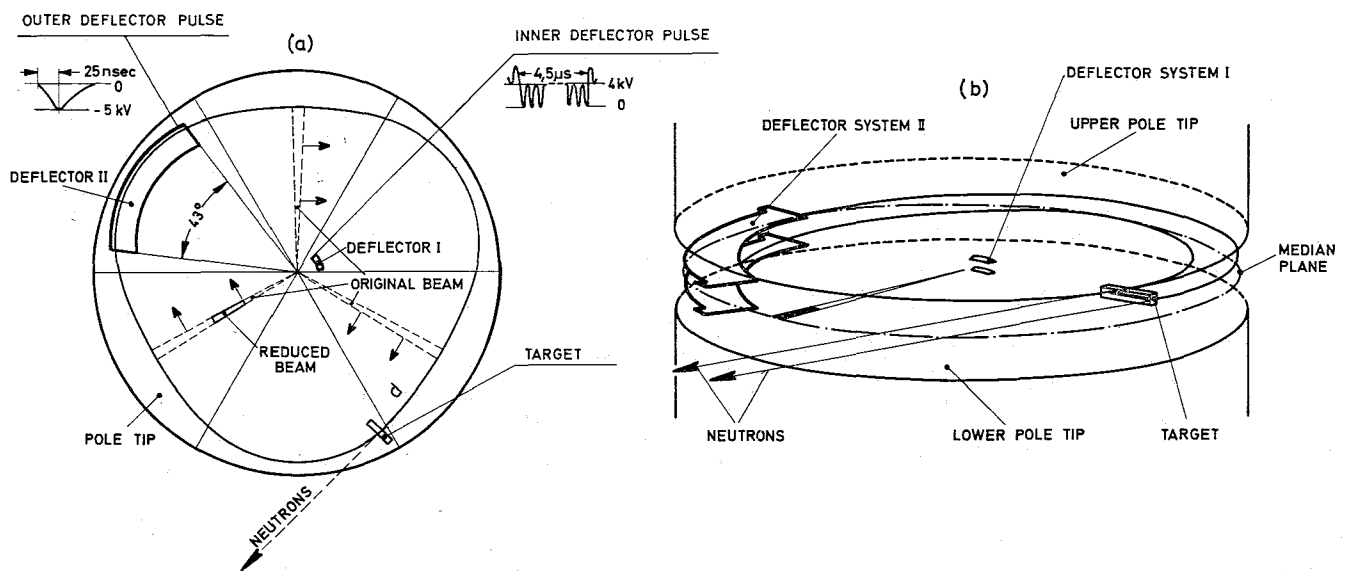


Fig. 1. Scheme of the bunching deflection system. (a) Top view. (b) Schematic drawing.

upper part of Fig. 1. A more detailed description follows in the next subsection.

A second pair of deflector plates is located at a mean radius of 980 mm and serves to deflect simultaneously the whole set of microstructure pulses to a neutron target positioned above the median plane of the cyclotron. At the time of deflection the entire bunch is distributed over several centimeters in radius. Before striking the target, the deflected beam completes almost an additional revolution.

For deflection a fast, high voltage pulse is applied to the deflection plates of system II (see Fig. 1).

It is evident from this description that such a system will produce single neutron pulses which are comparable in width with the microstructure pulses while the burst intensity is increased by a factor of about 50 (the number of microstructure pulses in a bunch). The increase in intensity however is obtained at the expense of the homogeneity in the energy of the ions striking the target. But, since the cyclotron is used as a "white" neutron source, this additional energy spread is of no concern.

C. Beam Suppression

The minimum voltage to deflect the beam onto a back stop positioned 1 cm above the median plane is 4 kV. For elimination of two out of three microstructure pulses a sine wave as shown in Fig. 2(a) works if the following conditions are fulfilled: (i) the period is just three times the period of the cyclotron rf and, (ii) the deflection voltage at the times t_1 and t_2 is sufficient for deflection of the entire ion pulses.

In the upper part of Fig. 2(a) this situation is demonstrated. The first microstructure pulse passes the plates at a moment when the deflection voltage is zero. Consequently this pulse is not influenced by the deflector plates. The two succeeding microstructure pulses then will arrive after 30 and 60 nsec respectively and since condition (ii) is fulfilled they will be removed from the beam.

The principle of pulsing the remaining part of the beam is illustrated in Fig. 2(b). A constant deflection voltage which is switched off only during a short time, for example, 4.5 μ sec every 50 μ sec, is applied to the lower deflection plate.

The resulting beam reduction is shown in the upper part of Fig. 2(b). A periodic variation of the deflection voltage, which can be obtained by a superposition of the two shapes

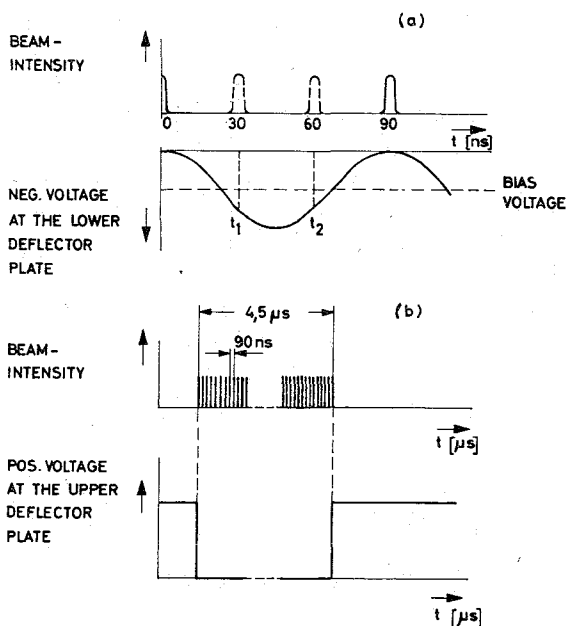


FIG. 2. Voltages of the deflector plates illustrating the principle of beam suppression. (a) Elimination of "two out of three" ion bunches. (b) Production of 4.5 μ sec pulses.

shown in Figs. 2(a) and (b), causes the abovementioned conditions (i) and (ii) to be fulfilled simultaneously.

D. Deflector Systems and Target Assembly

The inner deflector system, the plates with the beam stop, and the coaxial lines are shown in the photograph [Fig. 3(a)]. The plates, separated by 10 mm, are made of 2 mm thick tantalum to withstand high temperature without melting or evaporating. The plates are located at the fourth orbit near the center of the machine in a hill section of the magnet pole faces. For proper operation the radial extension of the plates was set at 4 cm. The azimuthal angle of 35° is limited largely by the space available in a hill section.

The inner deflector plates are supported by the rigid transfer line for the rf pulse. This consists of an air-dielectric coaxial transmission line between the wall of the vacuum tank and the pole tip. Inside the pole gap the transfer line passes into an 8×8 mm U-shaped waveguide located at the bottom pole face to prevent the ions from hitting this connector. The inner conductor is a silver-plated, 1 mm diam, quartz-insulated, copper conductor which is fixed by several Teflon anchor beads.

Line impedances are 235 or 135 Ω depending upon the different geometries of the waveguide. The rectangular pulse from the high voltage pulse generator [Fig. 2(b)] is fed to the plates by a Teflon-insulated Degussit tantalum conductor to hold the capacitance of the transfer line as low as possible. The water-cooled beam stop, made of 3 mm thick copper 8 mm in length and 10 mm high, is set directly above the entrance of the plates. In order to reduce secondary electron emission this copper bar was chromium-plated.

The outer deflector plates are 1 mm thick copper provided with water cooling. The plates which are shown in Fig. 3(b) extend between radii of 930 and 1030 mm corresponding to 40.5 and 50 MeV of deuteron energy respectively. The separation of the plates is 14 mm. The beam stop mounted directly above and below the entrance of the deflector serves to remove ions having a large vertical oscillation amplitude. The bottom plate of the deflector is grounded. The negative deflection voltage is applied to the upper plate which is supported by five aluminium bars insulated from the bottom plate by LAVA grade A insulators. Until 1966 the deflection plates were located in the hill section directly beyond the neutron target. In this position, however, the deuteron bunch could be peeled off partially, as it extended radially, by the edges of the deflector plates, giving rise to a background of additional neutron parasite pulses recurring at intervals of 90 nsec (the revolution period). This situation makes neutron time-of-flight work unfeasible. To avoid these effects a critical and time-consuming adjustment was necessary because of the limited space available between the magnet pole faces, and be-

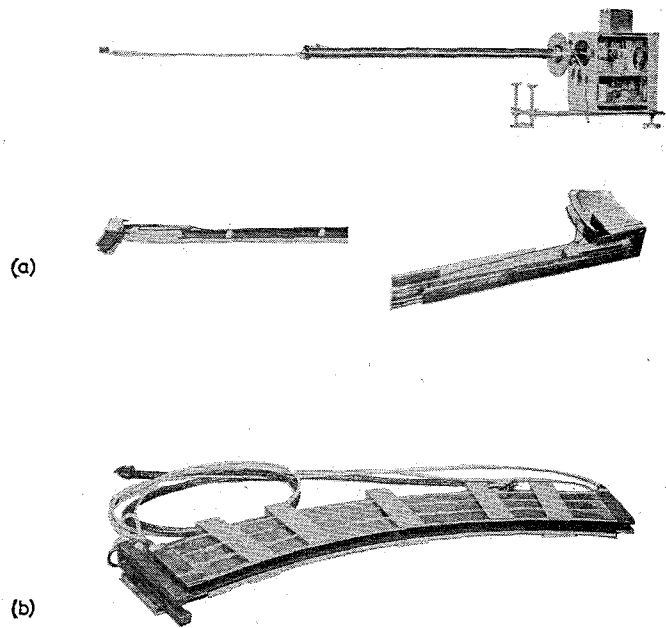


FIG. 3. (a) View of the deflector system I. (b) View of deflector system II.

cause of the relatively large overall cross section of the ion beam in the deflection area.

But now the plates are located in the last remaining hill section (Fig. 1). In this region a small fraction of the beam being peeled off does not matter because neutrons produced by the plate edges cannot enter the flight path. These are shielded by the collimators and the magnetic yoke of the machine. The optimal position for the deflector plates from a beam deflection point of view, however, is directly beyond the target. But the vertical displacement of the deuterons at the present target position is reduced only by about 20%, which loss could be compensated for easily by an equivalent increase of the deflection voltage.

For neutron production a natural uranium target 95 mm wide, 10 mm in height, and thick enough to stop 50 MeV deuterons, mounted on a 2 mm thick copper bar of the same dimensions, was used. If a time average of $3 \mu\text{A}$ of 45 MeV deuterons dissipate their energy in a target about 150 W heating is implied. Therefore a directly-cooled copper finger target is used. The uranium is covered by a 20μ thick copper foil to prevent fission products from contaminating the cyclotron tank. The target assembly is soldered on a copper block of 34 mm diam, 20 mm in length, and can be put in proper radial position by a remote controlled support.

Very small portions of the beam observable between the desired bunches give rise to parasite pulses when striking the copper block of the uranium target. To avoid such disturbances a so-called "dee-target" is used azimuthally far away from the uranium target. The dee-target is located

in such a way that the maximum ion radius is limited by the radial position of this target.

Neutron production at the dee-target is of no concern since these neutrons cannot reach the flight path. With this arrangement a total parasite pulse reduction was accomplished.

II. ELECTRONIC SYSTEM

The block diagram of the entire electronic system is shown in Fig. 4.

A. Timing

Figure 5 illustrates some of the several timing elements with reference to the basic cyclotron rf.

For proper operation of the deflection bunching system several timing conditions are necessary. A first condition concerns the inner deflector.

- (i) The phase correlation between the cyclotron rf and the 11 Mc sine wave (mentioned in the preceding section) must be accurately constant in time.

There are three further timing conditions concerning the pulse applied to the outer deflection plates.

- (ii) The deflection voltage must be applied when the deuteron bunch has reached the mean deflection radius, i.e., about $21 \mu\text{sec}$ (the acceleration time of 50 MeV deuterons) after deflector I has started releasing a deuteron bunch.
- (iii) The deflection pulse must rise from zero to its full value during that portion of the revolution period during which the bunch is outside the plates.

- (iv) The overall time jitter of the deflection pulse with respect to the isochronous acceptance angle must be small compared with the time needed for the ion bunch traversing the plates.

The width of the outer deflection pulse was set as small as possible ($\sim 30 \text{ nsec}$ FWHM), as this, in connection with the use of the dee-target, leads to a very effective background suppression. Therefore the time jitter with respect to the cyclotron rf of the deflection pulse must be less than a few nanoseconds.

The electronic circuits to fulfill the condition (i) are shown in the block diagram of Fig. 4. An accurately phased 11 Mc sine wave is achieved by mixing the output of the forced dumped 11 Mc oscillator with the 33 Mc rf provided by the rf generator of the cyclotron. It could be shown that the outgoing 11 Mc sine wave was strongly coupled to the cyclotron rf. In order to prove this the Lissajous figures formed by the 33 Mc rf and the 11 Mc reduced sine wave were observed over periods of days by use of a fast sampling oscilloscope. No phase shifts exceeding 1 nsec could be measured. The proper phase position for an accurate 3:1 suppression is selected by a manually variable delay line connected in series with the power amplifier. The reliability of the total system I was proved by measuring the time-of-flight spectrum obtained from a thick copper target. Figure 6 shows the time-of-flight spectrum when only the sine wave [Fig. 6(b)] or the pulsed sine wave [Fig. 6(c)] is applied to the inner deflector.

Figure 6(a) shows the situation when the deflection voltage is switched off. The diagrams in Fig. 6 require some comments. In this measurement a plastic scintillation counter was set to a distance of about 3 m from the target.

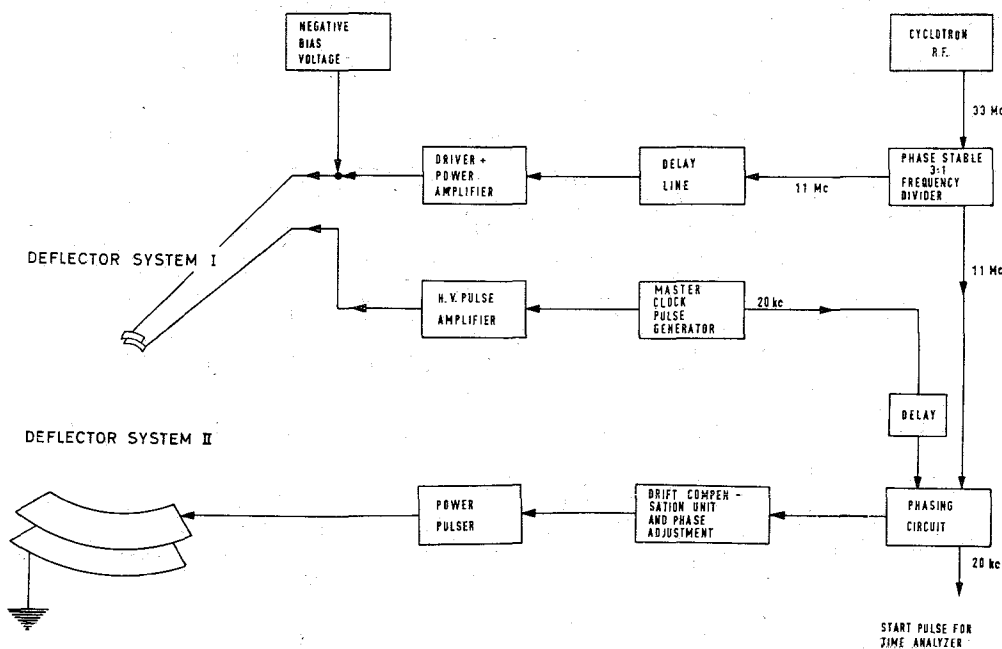


FIG. 4. Diagram of the deflection circuits.

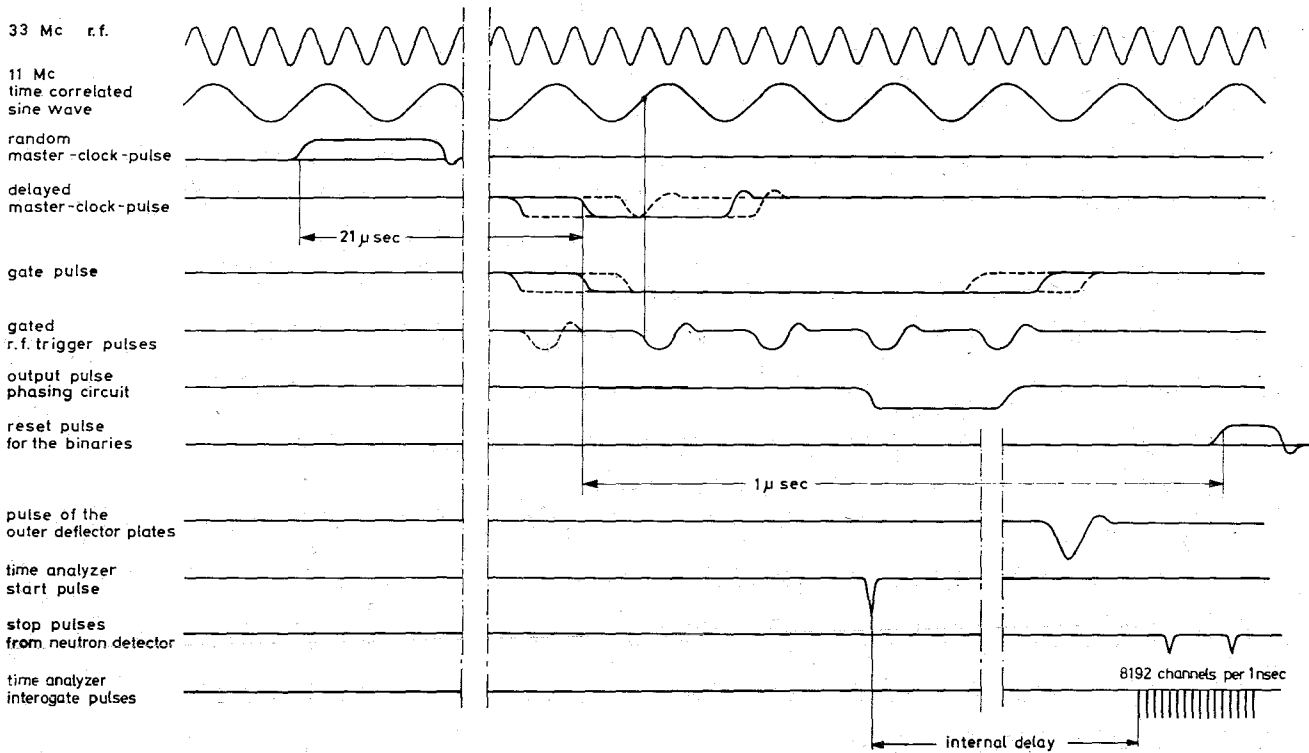


FIG. 5. Timing diagram for the time-of-flight spectrometer.

Therefore prominent peaks arise from the prompt γ rays of the target only, while most of the events due to neutron interactions in the scintillator appear as a slightly time-dependent background because of the strong overlapping of neutron spectra. For these runs no care was taken to obtain optimum timing conditions. Thus the width of the γ peaks does not reflect the actual neutron pulse width but rather is characteristic for the time resolution inherent to the recording equipment.

A circuit used to meet the timing requirements (ii)-(iv) is the phasing circuit (compare Fig. 5). The principle of operation is based on a circuit developed by Langsford *et al.*⁸ for the time-of-flight spectrometer in Harwell. The output signal from the 20 kc masterclock pulse generator is delayed by 21 μ sec. To obtain a time-correlated signal the 11 Mc pulses from the frequency divider are gated from the delayed masterclock pulse. Timing is arranged such that only a pulse train of four rf trigger pulses passes the gate.

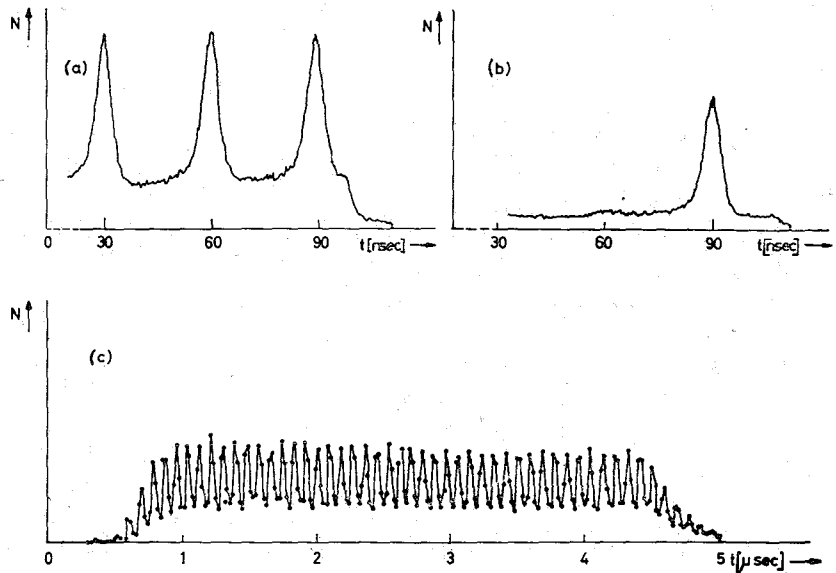


FIG. 6. Time-of-flight spectrum of prompt γ rays representing particle bunches. (a) Under normal operation. (b) With 3:1 ion pulse rate reduction. (c) Complete reduction to a bunch containing ≈ 50 microstructure ion pulses.

⁸ A. Langsford, D. E. Dolley, G. B. Huxtable, Nucl. Instr. Meth. 33, 57 (1965).

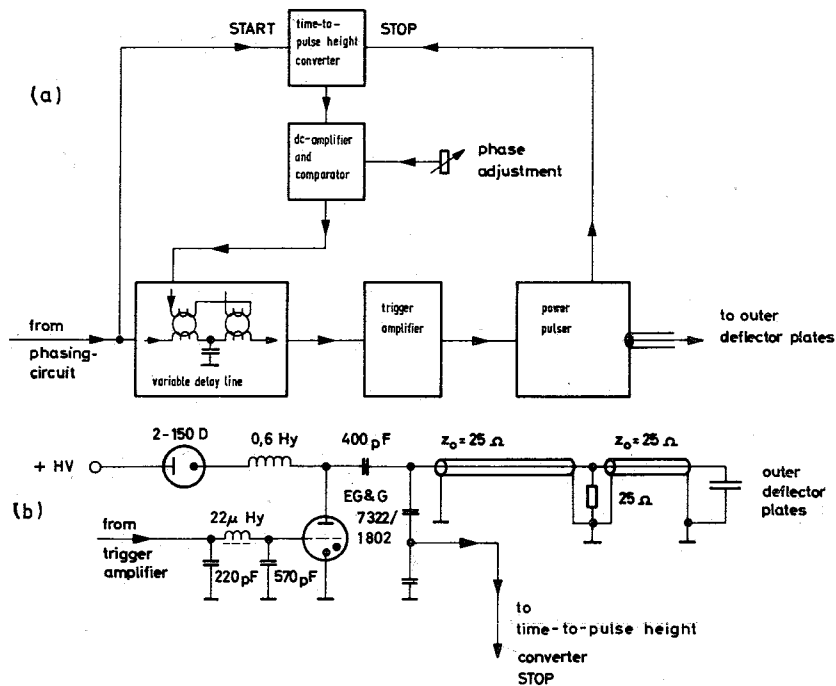


FIG. 7. Power pulse generator and long term drift-compensation unit. (a) Block diagram. (b) Power pulser circuit diagram.

From each pulse train the second pulse is selected as a time reference by two binaries. By this procedure the time jitter introduced to the first and the last pulses because of the finite rise and decay time of the gate pulse is eliminated. As the time distribution of the gate pulse with respect to the trigger pulse necessarily must be random there is a non-zero probability that either five or only four rf tunnel diode pulses pass the gate. If the binaries are not reset each after a pulse train has been accepted, the mentioned selection does not work and gives rise to uncorrect timing. To avoid complication an additional reset signal is provided from a reset pulse generator. By this signal all the flip-flops are reset 1 μ sec after an output signal is delivered. Using this phasing circuit an overall time jitter of less than 1 nsec was obtained.

B. Power Pulse Generator and Long Term Drift Compensation Unit

The block diagram of the power pulse generator is shown in Fig. 7(a). During the early runs difficulty was experienced in compensating the long term drift introduced generally by hydrogen thyratrons. Now the long term drift is compensated by a regulated variable delay line connected in series with the pulse generator circuit so that the transit time through the combined system can be held constant. The principle of operation⁹ shown in Fig. 7(a) is as follows: the delay network consists of constant capacitances and variable inductances. The resulting time delay from the compensation unit and the pulse generator is controlled

⁹ A. Ernst, H. Unseld, and S. Cierjacks, *Physik. Verhandl.* 17, 15 (1966).

by a time-to-pulse height conversion system. The obtained pulse height is transformed into an amplitude proportional direct current (independent of input frequency) which is compared with an equilibrium value. This direct current is used for premagnetization of the magnetic ring cores of which the second winding serves as the inductance in the low pass delay network. With this technique the resulting long term drift could be reduced to about 1–2 nsec during long operation periods of several weeks.

In Fig. 7(b) the power pulser circuit diagram is shown. The main components of the pulser are an EGG 1802 hydrogen thyatron, a 500 pF capacitor, a 25 Ω transferline, and a water-cooled, 25 Ω terminator. The thyatron is supplied with 5–8 kV dc through a 1 H inductance and a 2–150 D diode. As the deflector plates represent a 400 pF capacitance, a 400–650 A peak pulse current is necessary. With respect to the high repetition rate of 20 kc the thyatron operates at the upper limit of its capability.

III. PERFORMANCE OF THE SPECTROMETER

A. Geometry of the System

The geometry of the neutron time-of-flight spectrometer is shown in Fig. 8. The air-conditioned detector cabin is at the end of a 57 m flight path. The vacuum channel consists of single iron tubes 6 m in length and 1 m in diameter and is evacuated by a combined system of a rotary and a Roots pump. At operating condition pressures of several 10^{-2} Torr were achieved, which is sufficient for the experiments. There are two collimators in the flight path defining a narrow neutron beam with a solid angle of about 2×10^{-6} sr.

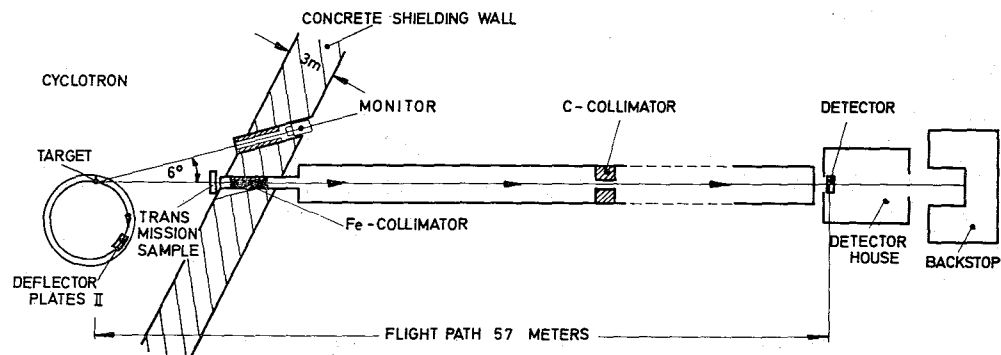


FIG. 8. Geometry of the Karlsruhe isochronous cyclotron time-of-flight spectrometer (top view).

The first collimator (2 m of iron) passes through the wall of the cyclotron building at the median plane height, 2.50 m above ground. The second, a graphite collimator, 75 cm in length, is located 37 m from the target and is positioned inside the vacuum tube. Graphite shielding material was chosen because of weight considerations.

Neutrons are detected by a proton recoil liquid scintillator NE 213 (9 cm diam and 1 cm thick). This detector is provided with a zero-crossover time pick-up circuit which was developed by Haase and Brückmann.¹⁰ For a 1:50 dynamic range a time resolution of 1.2 ± 0.2 nsec has been obtained with a ^{60}Co γ source.

For the purpose of beam monitoring a smaller liquid scintillator NE 213 mounted on a 56 AVP photomultiplier provided with pulse shape discrimination is placed at a second neutron beam at a small angle of 6° to the main flight path.

The two power pulse generators for the deflectors are placed as close as possible to the cyclotron. When not in use these can be removed from their operating position. The whole deflection system is controlled from an experimental room inside the cyclotron building where most of the electronic circuitry is placed.

Only the neutron detector and the power supplies are placed in the detector station. A normalized time signal from the detector is transferred to the cyclotron building via a Flexwell 9.5 mm 50Ω cable.

B. Time Analyzer System and Data Acquisition

For the first transmission measurements in 1966 an Intertechnique digital time sorter, with a maximum of 32 000 channels and a 1 nsec minimum channel width, was employed. The output bits of the analyzer were transferred from the cyclotron building to the MIDAS data acquisition system,^{11,12} located at the Karlsruhe FR2 reactor, and were accumulated in the memory of the on-line computer CDC 160 A. During that time the operation of the system

¹⁰ H. Brückmann, E. L. Haase, W. Kluge, and L. Schänzler, Nucl. Instr. Meth. (to be published).

¹¹ G. Krüger and G. Zipf; KFK-Rep. 371.

¹² G. Krüger, G. Dimmler, G. Zipf, H. Hanak, and R. Merkel, Kerntechnik 8, 273 (1966).

was controlled simultaneously at the cyclotron building by means of a live display.

Now a digital time analyzer (Laben UC-KB)^{13,14} with 262 144 channels at maximum is available which can accept several stop pulses per burst. This time sorter is connected with the new CDC 3100 data acquisition system¹⁵ at the cyclotron. The channel width of the time sorter can be selected in binary steps from 0.5 nsec to any upper limit. The start signal can be delayed in steps of ~ 1 μsec from 0 to 127 μsec . Therefore it is possible to fix the desired energy range arbitrarily in the preselected intervals.

The output signals from the time sorter are fed *via* a four word fast buffer to the CDC 3100 with a present memory capacity of 16 k 24 bit words for program and storage.

For transmission measurements which were conducted with a range of about 8 μsec and a channel width of 1 nsec the storage capacity was not sufficient to accumulate all data for "sample in" and "open beam" position in the memory directly. After preaccumulation in the computer memory the events are stored on magnetic tape and accumulated separately after the runs. Because of the high input rate of up to 1×10^4 counts/sec only on-line operations, e.g., shifting the γ peak, live display and registration of the dead time constants are possible because of the limited storage capacity. Operations such as octal-to-decimal conversion, combining events of similar runs, background subtraction, dead time corrections, and assignment of the particle energy are performed with an IBM 7074 data processing system.

C. Characteristic Features of the Spectrometer

1. Neutron Spectrum

A typical time-of-flight spectrum obtained for thick uranium targets using a NE 213 liquid scintillator at the end of the flight path is shown in Fig. 9(b). In Fig. 9(a)

¹³ I. De Lotto, E. Gatti, and F. Vaghi, in *Proceedings of the Conference on Automatic Acquisition and Reduction of Nuclear Data*, K. H. Beckurts *et al.*, Eds. (Gesellschaft für Kernforschung m.b.H., 1964), p. 291.

¹⁴ C. Cottini, I. De Lotto, D. Dotti, E. Gatti, and F. Vaghi, *Energia Nucl.* 14, 704 (1967).

¹⁵ D. Jenet, private communication.

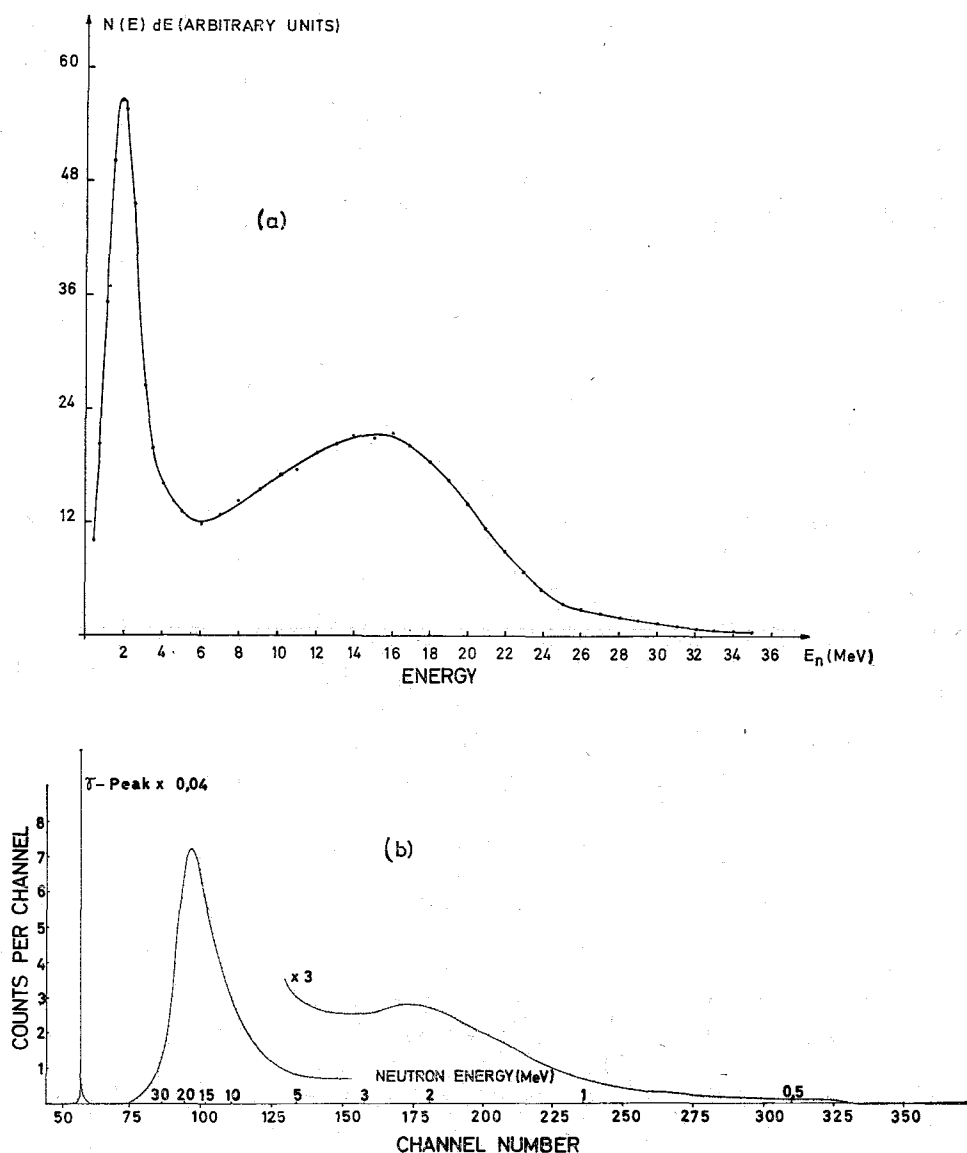


FIG. 9. (a) Typical energy spectrum. (b) Typical neutron time-of-flight spectrum.

this spectrum is shown as a function of energy. The detector threshold was set to a value corresponding to 250 keV neutron energy. In this figure an average of 20 channels of the original spectrum is shown for clearness. The maximum at about 16–20 MeV is mainly due to neutrons from deuteron break-up in the Coulomb field and at the nuclear surface. The energy distribution of neutrons in the forward direction for these processes can be explained to a first approximation by the expressions of Serber,¹⁶ who predicts a symmetrical energy distribution with a broad half width centered around half the bombarding deuteron energy. The position of the observed maximum which is shifted to a lower energy can be explained by the following two facts: (i) as a thick target is used deuterons with energies between 0–50 MeV contribute to the total neutron yield; and (ii) for deuteron break-up processes at the nuclear

¹⁶ R. Serber, Phys. Rev. **72**, 1008 (1947).

surface the actual deuteron energy is decreased by the amount of the Coulomb energy. The distribution at energies smaller than ~6 MeV mainly represents the distribution of neutrons from evaporation and fission processes. These well known evaporation spectra¹⁷ show maxima at energies between about 0.5–2 MeV depending slightly upon the excitation energy of the compound nucleus. For energies above the maximum the neutron yield decreases nearly exponentially (this description is to a first approximation also true for fission spectra).

2. Energy Resolution

The energy resolution of the spectrometer has been determined both by the time distribution of γ rays within the peak of the prompt γ rays from the target and by mea-

¹⁷ I. M. B. Lang and K. I. Le Couteur, Nucl. Phys. **14**, 21 (1959) and Proc. Phys. Soc. London **A67**, 586 (1954).

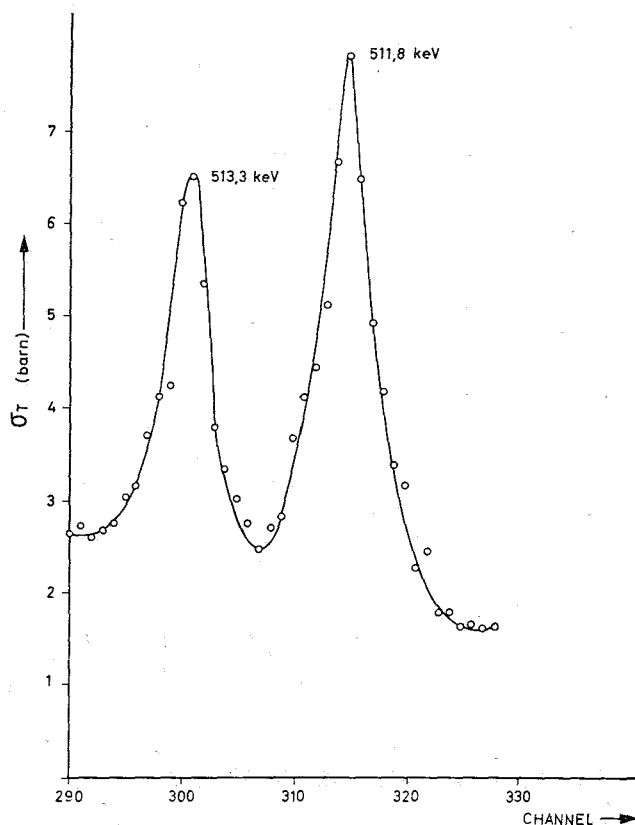


FIG. 10. σ_T for natural iron in the 510 keV region.

asuring the resonances of ^{56}Fe near 510 keV as shown in Fig. 10. There are two closely spaced resonances, as Beard¹⁸ has shown. The two resonances at about 512 keV were well resolved in our first measurements. From the measured half width of these resonances the resolution is seen to be at least equal to or better than 400 eV. From a calculation of the maximum cross section a resolution of about 200 ± 50 eV was deduced, assuming the 511.8 and 513 keV resonances to be $J = \frac{1}{2}$ and $J = \frac{3}{2}$ resonances respectively. The same value within the experimental uncertainty was obtained from the width and the shape of the prompt γ peak which reflects the time distribution of the neutron burst at the target plus any finite time resolution inherent in the recording equipment.

Table I shows the energy resolution obtainable under different conditions. The total neutron burst length was 1 nsec. The energy resolution which is derived from the neutron burst length is shown in the first column. This resolution can be achieved for small detectors (in connection with high speed photomultipliers). Large detector assemblies typically show a time resolution of ~ 1.8 nsec with a dynamical range of 1:2000. Under these conditions the energy resolution in a first approximation is due to the values shown in the second column. The third set indicates what reasonably is possible with an increased flight path of 180 m and

¹⁸ P. M. Beard, Ph.D. Thesis, Duke University, 1964 (unpublished).

TABLE I. Energy resolution of the Karlsruhe fast neutron time-of-flight spectrometer.

E_n (MeV)	57 m 1 nsec ΔE (keV)	57 m 2 nsec ΔE (keV)	180 m 1 nsec ΔE (keV)
0.5	0.17	0.35	0.055
1.0	0.49	0.98	0.16
2.0	1.4	2.8	0.44
4.0	3.9	7.9	1.2
5.0	5.5	11.0	1.7
10.0	15.5	31.0	4.9
20.0	43.9	87.7	13.9
30.0	80.7	161.4	25.5

with further effort to improve the time resolution for large detector assemblies.

The overall neutron intensity available from a thick uranium target has not yet been determined very accurately. However a rough calculation of the detector efficiency indicates a value of $5 \pm 2 \times 10^4$ neutrons/sec cm^2 above 250 keV neutron threshold at the end of the flight path. The characteristic features of the spectrometer are summarized in Table II.

TABLE II. Time-of-flight apparatus.

Flight path	57 m
Deflection radius	0.930 m (40.5 MeV deuterons) to 1.030 m (50 MeV deuterons)
Time resolution	(1 ± 0.3) nsec full width at half maximum
Energy resolution	200 ± 50 eV at 0.5 MeV (optimum)
Resolution of the spectrometer	0.025 nsec/m
Integrated neutron flux at 3 μA target current	$(5 \pm 2) \cdot 10^4$ neutrons- cm^{-2} -sec $^{-1}$ above $E_n = 250$ keV at 57 m

D. Examples of Operation

One of a series of results on the measurements of total neutron cross sections may demonstrate the overall performance of the spectrometer. In Fig. 11 the results for calcium in the energy region between 1-2 MeV measured with a 1-2% statistical accuracy are shown. The most extensive measurement with which the present data can be compared are those given in the Brookhaven compilation¹⁹ and by Deconninck²⁰ (not shown). The present data exhibit considerably more structure than appears in the earlier work. The difference can be ascribed chiefly to the difference in the energy resolution. If the curves in Fig. 11 are smoothed by using an average interval equivalent to the energy spread of the previous experiments, the remaining structure agrees with the observed values in the other laboratories. The average cross sections agree within the uncertainty of the measurements in the whole energy range although the present data are ~ 1 -2% higher.

¹⁹ D. I. Hughes, B. A. Magurno, and M. K. Brussel, BNL 325 Suppl. No. 1, 2nd ed. (Jan. 1, 1960).

²⁰ G. Deconninck, and M. Husain, Ann. Soc. Sci. Bruxelles (T80) II, 185 (1966).

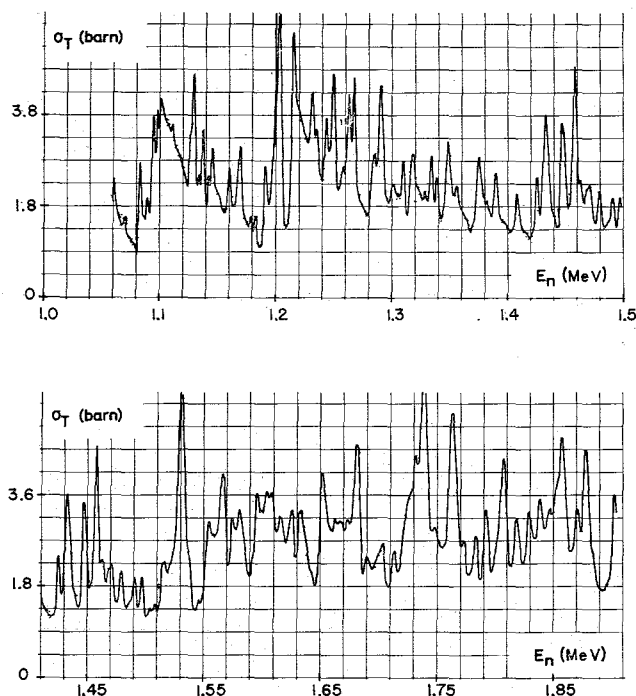


FIG. 11. Total neutron cross section of calcium.

IV. Improvements

With respect to neutron production and high resolution aspects the Karlsruhe time-of-flight facility will be improved as follows: first, an increase of the flight path to a total length of 180 m is under way. The expected energy resolution with the increased flight path will exceed 0.01 nsec/m (compare Table I) which is mainly important in the energy range above several megaelectron volts.

Second, an increase of the pulse repetition rate from 20 to about 200 kc is in progress. As this cannot be accomplished with the existing deflection facility a reconstruction of the outer deflection system is necessary. A new pulse generator for high recurrence frequencies has been developed using microwave power tubes instead of the thyratron.

Additionally it has been shown that a suitably shaped upper deflection plate acting as a strip-line element would reduce the power requirements for beam deflection considerably.²¹

²¹ H. Unseld, *Proceedings of the 'Fachtagung Antennen und elektromagnetische Felder' der NTG und U. R. S. I. Darmstadt, Oct. 1967* (to be published).

With the present flight path, repetition rates up to 160 kc are acceptable if measurements are restricted to a lower energy threshold of ~ 500 keV. For unmoderated neutron spectra a restriction to a neutron energy of several hundred kiloelectron volts seems reasonable since the intensity per channel decreases rapidly and background difficulties arise at lower energies.

In addition the construction of remotely controlled deflector plates is under way. From this provision it is expected that the bunching deflection system can be left in the cyclotron tank during periods when the system is not in operation.

No strong effort has yet been made to decrease the neutron burst length. The obtained burst length of 1 ± 0.3 nsec results mainly from the microstructure pulse width (~ 0.8 nsec) of the cyclotron which depends mainly upon the starting conditions of the ions from the source. The main parameters are the ion source position and the rf amplitude.²² It should be mentioned that any improvement of the phase acceptance angle results in a considerable decrease of the average intensity. Another component contributing to the actually obtained pulse width of the neutron burst is the radial particle phase position which changes slightly with the radius if particles proceed through larger radii (for an unfavourable trim coil adjustment phase shifts up to a few nanoseconds have been observed²²). Based on these arguments there seems to be little chance to considerably decrease the neutron burst length in the present situation.

ACKNOWLEDGMENTS

The project arose out of discussion with Prof. K. H. Beckurts. The help provided by all members of the cyclotron crew headed by Dr. G. Schatz and F. Schulz is gratefully acknowledged.

We are indebted to the "data handling group" of our institute. Primarily, we would like to thank G. Gagel who designed and built all the hardware for computer connections, and Mrs. D. Jenet who provided us with several computer programs for the CDC 160 A and the CDC 3100 acquisition systems.

²² D. Hartwig, W. Linder, M. Lösel, G. Schatz, and H. Schweikert, KFK-Rep., to be published.